Empirical assessment of the detection efficiency of CR-39 at high proton fluence and a compact, proton detector for high-fluence applications
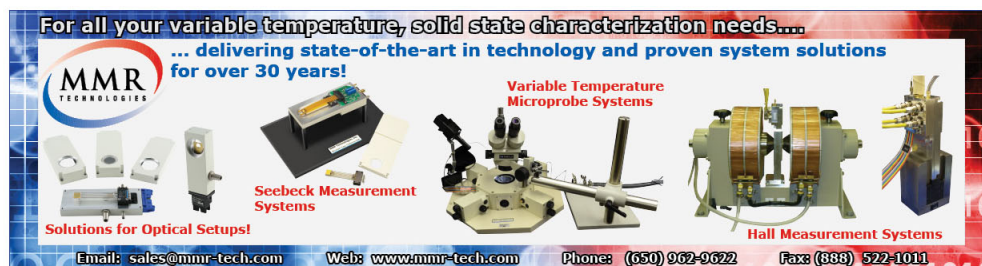
M. J. Rosenberg, F. H. Séguin, C. J. Waugh, H. G. Rinderknecht, D. Orozco, J. A. Frenje, M. Gatu Johnson, H. Sio, A. B. Zylstra, N. Sinenian, C. K. Li, R. D. Petrasso, V. Yu. Glebov, C. Stoeckl, M. Hohenberger, T. C. Sangster, S. LePape, A. J. Mackinnon, R. M. Bionta, O. L. Landen, R. A. Zacharias, Y. Kim, H. W. Herrmann, and J. D. Kilkenny

Empirical assessment of the detection efficiency of CR-39 at high proton fluence and a compact, proton detector for high-fluence applications

M. J. Rosenberg,[1,a)] F. H. Séguin,[1] C. J. Waugh,[1] H. G. Rinderknecht,[1] D. Orozco,[1] J. A. Frenje,[1] M. Gatu Johnson,[1] H. Sio,[1] A. B. Zylstra,[1] N. Sinenian,[1] C. K. Li,[1] R. D. Petrasso,[1] V. Yu. Glebov,[2] C. Stoeckl,[2] M. Hohenberger,[2] T. C. Sangster,[2] S. LePape,[3] A. J. Mackinnon,[3] R. M. Bionta,[3] O. L. Landen,[3] R. A. Zacharias,[3] Y. Kim,[4] H. W. Herrmann,[4] and J. D. Kilkenny[5]

[1]*Plasma Science and Fusion Center, Massachusetts Institute of Technology, Cambridge, Massachusetts 02139, USA*
[2]*Laboratory for Laser Energetics, University of Rochester, Rochester, New York 14623, USA*
[3]*Lawrence Livermore National Laboratory, Livermore, California 94550, USA*
[4]*Los Alamos National Laboratory, Los Alamos, New Mexico 87545, USA*
[5]*General Atomics, San Diego, California 92186, USA*

CR-39 solid-state nuclear track detectors are widely used in physics and in many inertial confinement fusion (ICF) experiments, and under ideal conditions these detectors have 100% detection efficiency for ∼0.5–8 MeV protons. When the fluence of incident particles becomes too high, overlap of particle tracks leads to under-counting at typical processing conditions (5 h etch in $6N$ NaOH at 80 °C). Short etch times required to avoid overlap can cause under-counting as well, as tracks are not fully developed. Experiments have determined the minimum etch times for 100% detection of 1.7–4.3-MeV protons and established that for 2.4-MeV protons, relevant for detection of DD protons, the maximum fluence that can be detected using normal processing techniques is $\lesssim 3 \times 10^6$ cm^{-2}. A CR-39-based proton detector has been developed to mitigate issues related to high particle fluences on ICF facilities. Using a pinhole and scattering foil several mm in front of the CR-39, proton fluences at the CR-39 are reduced by more than a factor of ∼50, increasing the operating yield upper limit by a comparable amount. © *2014 AIP Publishing LLC*. [http://dx.doi.org/10.1063/1.4870898]
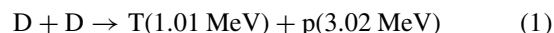
I. INTRODUCTION

CR-39 solid-state nuclear track detectors are used in a variety of applications to detect charged particles based on damage trails left by incident particles depositing energy in the material.[1] In inertial confinement fusion (ICF) research, CR-39-based diagnostics measure the fusion yield, ion temperature, areal density, and burn profile in imploding capsules,[2–6] as well as electric and magnetic fields in laser-driven high-energy-density physics experiments.[7–9]

Under normal conditions, tracks are counted individually with 100% detection efficiency with very little systematic error. However, when particle fluences become too high, tracks can overlap in such a way that detection software cannot distinguish them, and tracks are either not counted or are under-counted (when multiple tracks are recorded as zero or one track).[10] This situation can arise especially on high-yield applications such as exploding-pusher implosions for diagnostic calibration at the National Ignition Facility (NIF)[11] or the OMEGA laser facility[12] where detector positions are fixed.
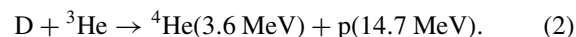
Previous studies of the usage of CR-39 detectors in high-fluence applications have focused on details of track formation[13] and models of track overlap probability,[10, 13, 14] as well as the optical properties of CR-39 in the highly saturated regime.[15]

This work seeks to determine empirically the minimum etch time required for all tracks to become visible, to as-

sess the fluence upper limit for 100% detection on CR-39 specifically for protons, and to establish a technique for extending the yield upper limit of operation of CR-39-based measurements by reducing the fluence at the CR-39 surface. Though this work specifically discusses proton detection, it can be extended to other energetic charged particles, including deuterons, tritons, and alpha particles. This study focuses on the protons produced in DD and D^{3}He reactions

$$D + D \rightarrow T(1.01\,\text{MeV}) + p(3.02\,\text{MeV}) \qquad (1)$$

and

$$D + {}^3\text{He} \rightarrow {}^4\text{He}(3.6\,\text{MeV}) + p(14.7\,\text{MeV}). \qquad (2)$$

These reactions are used to characterize the yield, ion temperature, and ρR in certain classes of ICF implosions.

The paper is organized as follows: Sec. II discusses the difficulty of proton detection using CR-39 under high-fluence conditions and establishes lower limits on etch time and upper limits on proton fluence for 100% detection efficiency; Sec. III presents a new instrument for mitigating high proton fluence and shifting the fluence upper-limit to extend the yield operating range for DD-proton yield measurements; Sec. IV discusses the results and potential applications; and Sec. V presents concluding remarks.
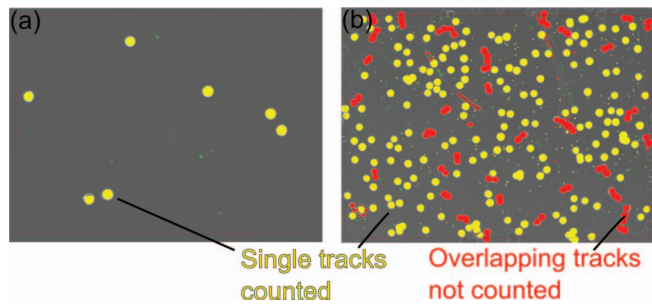
a)Electronic mail: mrosenbe@mit.edu

© 2014 AIP Publishing LLC

FIG. 1. Microscope images of proton tracks at (a) a moderate fluence of 5×10^3 cm^{-2}, after a 6-h etch, and (b) a high fluence of 2.4×10^5 cm^{-2}, after a 5-h etch. At a high fluence and long etch time, track overlap causes undercounting of proton tracks and an erroneously low yield measurement. The yellow single tracks are counted, but the red tracks are ignored.

II. HIGH-FLUENCE PROTON DETECTION USING CR-39

Charged particles incident on the CR-39 leave trails of damage in the form of broken molecular bonds as energy is deposited along their trajectories. Etching the CR-39 in a $6N$ solution of sodium hydroxide (NaOH) at $80\,^\circ$C reveals the damage trails such that their diameters are of order micrometers and they are visible using standard microscope equipment with a typical magnification of $40\times$. Individual tracks are identified and recorded for use in charged-particle diagnostics. Protons of energy $\sim$0.5–8 MeV are detectable with a 100% efficiency under normal fluence circumstances.[4] The diameter of proton tracks has been determined empirically to be inversely correlated with the incident proton energy above $\sim$0.5 MeV,[16] such that lower-energy protons leave larger tracks.[4,17] When the particle fluence is high enough that tracks begin to overlap, they are not all counted, introduc-

ing errors into measurements that rely on the absolute number or diameter of particle tracks. Figure 1 illustrates proton tracks after 5–6 h of etching under a $40\times$ magnification. At a moderate fluence of 5×10^3 cm^{-2} (6 h of etching), tracks are well-separated and are counted individually with insignificant overlap. At a high fluence of 2.4×10^5 cm^{-2} (5 h of etching), many of the tracks (red) are overlapping and are not recorded by the track detection software. Algorithms to correctly detect and identify multiple overlapping tracks have yet to be developed.

Experiments to assess the CR-39 detection efficiency under high-fluence conditions have been performed at the MIT Linear Electrostatic Ion Accelerator (LEIA),[18] as well as at OMEGA and the NIF. High fluence experiments have been conducted using aluminum-filtered CR-39 with DD and D^{3}He protons at a uniform track diameter and on wedge-filtered CR-39 with a continuum of D^{3}He-proton track diameters. As track overlap depends on the diameter of the proton tracks as well as their fluence, protons of different energies experience different degrees of overlap (lower-energy protons leave larger tracks and are more susceptible to overlap) and, consequently, have different fluence upper limits.

A. Flat-filtered CR-39

Figure 2 illustrates the under-counting problem of protons of different energies as a function of etch time in high fluence conditions. On OMEGA shot 62409, a thin glass shell filled with D^{3}He gas imploded with 30 kJ of laser energy in a 1-ns pulse, DD and D^{3}He protons were detected by CR-39 filtered by flat pieces of aluminum. With detectors at 175 cm away from the target, the 7.6×10^{10} DD protons and 1.4×10^{11} D^{3}He protons were measured at a fluence of
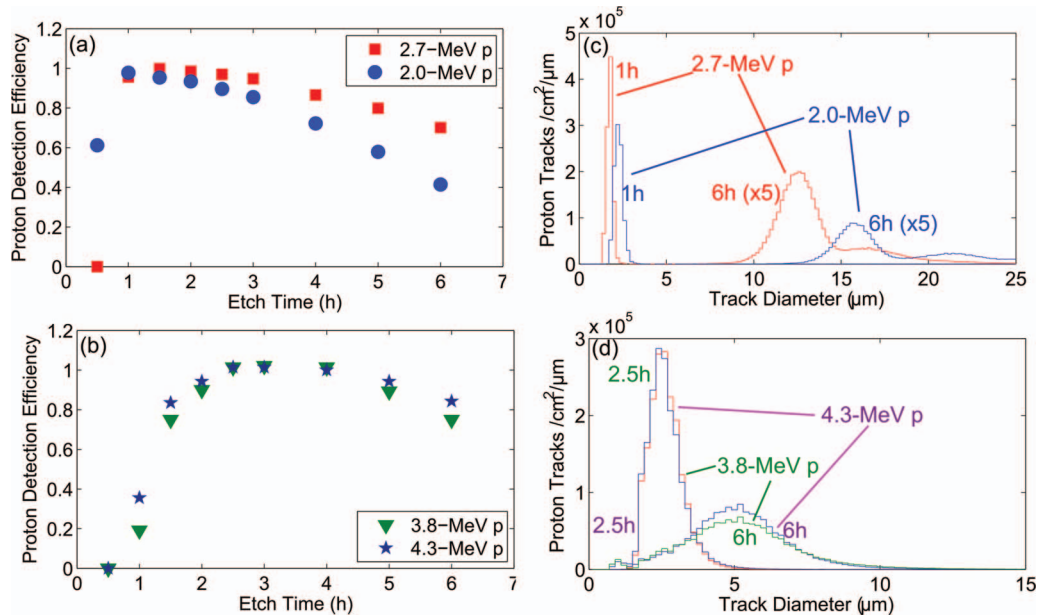

FIG. 2. Detection efficiency for (a) 2.0- and 2.7-MeV protons at a fluence of 2.0×10^5 cm^{-2} and (b) 3.8- and 4.3-MeV protons at a fluence of 3.7×10^5 cm^{-2}. These data illustrate the under-counting of protons at short etch times, before all tracks are visible using the $40\times$ magnification, and at long etch times, as track overlap prevents the counting of all proton tracks. The corresponding diameter histograms for (c) 2.0- and 2.7-MeV protons and (d) 3.8- and 4.3-MeV protons illustrate the growth and increasing overlap of tracks at long etch times. The long high-diameter tails for the 2.0- and 2.7-MeV-proton tracks in (c) are a consequence of multiple overlapping tracks being interpreted as one large track.

2.0×10^5 cm^{-2} and 3.7×10^5 cm^{-2}, respectively. DD protons (Figure 2(a)) were ranged through either 25 μm or 50 μm of Al, ending up at 2.7 or 2.0 MeV. D^{3}He protons were ranged through either 200 μm or 175 μm of Al, as well as $\sim$1500 μm of CR-39, ending up at 3.8 or 4.3 MeV.

At short etch times, not all of the DD-proton tracks were visible, such that after a 0.5 h etch, only 61% of the larger, 2.0-MeV-proton tracks and virtually none of the smaller 2.7-MeV-proton tracks were visible (Figure 2(a)). By a 1-h etch, the inferred yield reached a maximum, as 100% of the tracks are being counted and track overlap is not yet significant. As the etch time is increased further, the inferred yield begins to drop – more rapidly for the larger, 2.0-MeV-proton tracks – as tracks begin to overlap and are not counted. By a 6-h etch, only 42% of the 2.0-MeV-proton tracks and 70% of the 2.7-MeV-proton tracks are correctly counted. These results are also reflected in the diameter histograms (Figure 2(c)), as the 2.0-MeV protons are at larger diameters and more prone to track overlap, showing at a 6-h etch a rather long high-diameter tail due to multiple overlapping tracks that are recorded as a single, large track. The trend of detection efficiency with etch time is similar for higher-energy, smaller-diameter D^{3}He protons. At a 1-h etch, only 19% of 3.8-MeV-proton tracks and 35% of 4.3-MeV-proton tracks are counted (Figure 2(b)). Detection of 100% of the protons only occurs by a 2.5-h etch – as evidenced by the plateau in detection efficiency – and, subsequently, track overlap diminishes the inferred yield at longer etch times. At a 6-h etch, 73% of 4.3-MeV-proton tracks and 83% of 3.8-MeV-proton tracks are counted. Because of the relatively small difference in track diameters between 3.8-MeV protons and 4.3-MeV protons (Figure 2(d)), as the CR-39 response does not change substantially at high energy, there is not as much of a difference in the incidence of track overlap and reduction of detection efficiency.

These data can also be used to assess a model of track overlap, which predicts track overlap to increase linearly with the proton fluence and with the effective area of an average track.[10] For the 3.8-MeV-proton data at a 6 h etch shown in Figures 2(b) and 2(d), with a fluence of 3.7×10^5 cm^{-2} and a mean track diameter of 5.5 μm, the model predicts that 70% of tracks are not overlapping. This prediction is in excellent agreement with the 73% detection efficiency that was measured. However, the model has difficulty under conditions of extreme overlap, such as the 2.0-MeV-proton data at a 6-h etch. At a fluence of 2.0×10^5 cm^{-2} and a mean track diameter (for the main peak) of 16 μm, the model predicts that only 22% of tracks are not subject to overlap, much lower than the measured detection efficiency of 42%. It is likely that a substantial fraction of the recorded tracks are actually multiple overlapping tracks recorded as a single track. This effect is encapsulated in the long high-diameter tails at a 6-h etch in Figure 2(c).

Experiments on the MIT LEIA, illustrated schematically in Figure 3 more closely assess the under-counting of proton tracks at short etch times. In these experiments, a deuterium beam incident on a ^{3}He-doped ErD$_2$ target produces DD and D^{3}He fusion products, which are detected by a surface barrier detector (SBD). The SBD provides confirmation of the
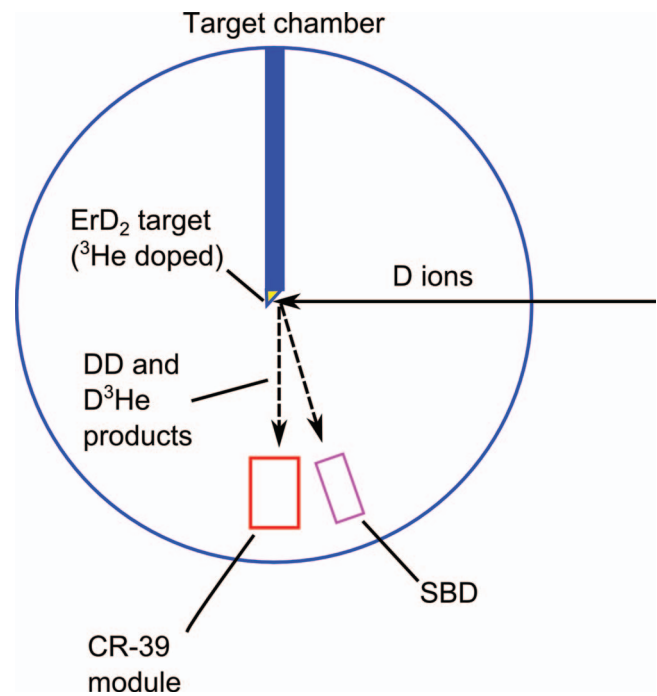

FIG. 3. Diagram of experiments on the MIT Linear Electrostatic Ion Accelerator (LEIA). A deuteron beam impinges on a ^{3}He-doped, ErD$_2$ target, generating DD and D^{3}He protons, which are detected by both a surface barrier detector (SBD) and CR-39 detectors.

expected nuclear production rate, for comparison to CR-39-based measurements. Figure 4 shows measured proton fluences on the CR-39 as a function of etch time at fluences of (a) 3.2×10^5 cm^{-2}, (b) 6.4×10^5 cm^{-2}, and (c) 3.0×10^6 cm^{-2}. The actual fluences were measured with a SBD, providing an independent measure for comparison to the CR-39 data. The data indicate that by etch times of 0.75 h or 1 h, all of the 1.7-MeV- and 2.4-MeV-proton tracks are counted at fluences of 3.2×10^5 cm^{-2} and 6.4×10^5 cm^{-2}. However, at a 0.5 h etch, when using a $40\times$ magnification, only 17% of 2.4-MeV-proton and 87% of 1.7-MeV-proton tracks are counted. At the short etch times necessary to avoid track overlap in high fluence conditions, some of the proton tracks are not visible under typical scanning conditions. Use of the $100\times$ magnification allows all tracks to be recorded at a 0.5 h etch; however, scanning with the $100\times$ objective is very time-consuming and is generally avoided.

These experiments demonstrate that when scanning with the $40\times$ objective, an etch time of 1 h is necessary to reveal all of the proton tracks. Thus, if track overlap becomes significant at earlier than a 1 h etch, normal processing will not be able to achieve 100% detection efficiency. For example, at a fluence of 3.0×10^6 cm^{-2}, by a 1 h etch, track overlap is already significant enough to reduce the detection efficiency to 88%. These results establish that at fluences at or above 3.0×10^6 cm^{-2}, 2.4-MeV protons cannot be counted at 100% efficiency using normal CR-39 processing techniques. This limit will also apply for protons at a lower energy, which have larger diameters and are therefore more susceptible to track overlap.[10]
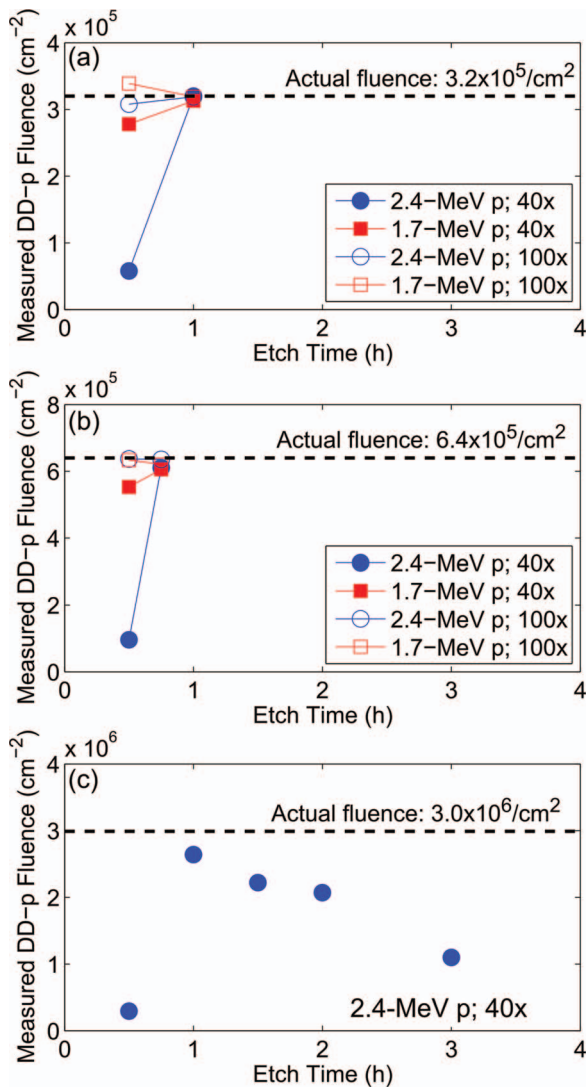
FIG. 4. Measured DD-proton fluence as a function of etch time at fluence of (a) 3.2×10^5 cm^{-2}, (b) 6.4×10^5 cm^{-2}, and (c) 3.0×10^6 cm^{-2}. The actual fluence was measured using the SBD. Measurement uncertainty is approximately the size of the symbols.

B. Wedge-filtered CR-39

CR-39 proton data obtained with wedge-range-filter (WRF) proton spectrometers[4,19,20] also display track overlap problems under certain conditions, which can impact measurements of yield, burn-averaged ion temperature, and areal density. NIF D^{3}He exploding pusher shot N110722 produced a yield of 1.35×10^{10} protons, and WRFs positioned 50 cm from the implosion were exposed to a fluence of 4.3×10^5 cm^{-2} protons. Images of tracks corresponding to protons likely at an energy of $\sim$2–3 MeV incident on the CR-39, after being ranged through the aluminum wedge, are shown in Figure 5. After 2.5 h of etching (Figure 5(a)), only 4% of proton tracks are overlapping, while after 5 h of etching (Figure 5(b)) 48% of tracks are not counted due to track overlap.

The inferred detection efficiency for 14.4-MeV protons ranged through the WRF are shown as a function of etch time for N110722 and similar D^{3}He exploding pusher N121128 in
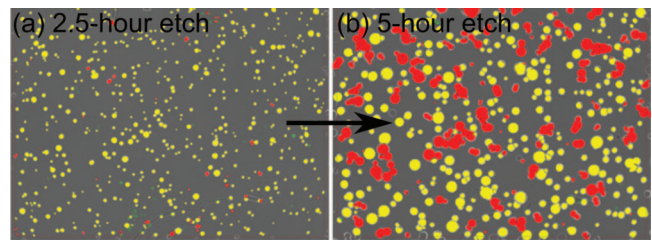

FIG. 5. Microscope images of D^{3}He proton tracks from the wedge-range-filter (WRF) spectrometer on NIF shot N110722 at (a) a 2.5-h etch, and (b) a 5-h etch. The WRF was positioned at 50 cm from the implosion, resulting in a fluence of 4.3×10^5 cm^{-2}. The yellow tracks are counted as single tracks and the red overlapping tracks are ignored. These tracks correspond to protons likely at an energy of $\sim$2–3 MeV incident on the CR-39, after being ranged through the aluminum wedge.

Figure 6. The tracks analyzed in the WRF data correspond to protons at an incident energy on the CR-39 of $\sim$1–4 MeV. Both pieces of data show track under-counting at short etch times, albeit much more severely in the N121128 data, with only 34% of the tracks recorded at a 1-h etch. This difference reflects differences in CR-39 sensitivity across different batches or individual pieces. The N110722 data, at a slightly lower fluence, have a more gradual decrease in the inferred yield and a more extended plateau, still counting 93% of its tracks by a 3.5-h etch. The N121128 data show a sharper retreat from the peak in the inferred yield, with an efficiency of 81% after a 3-h etch and 63% after a 5-h etch. The shape of the N121128 curve suggests that 6.5×10^5 cm^{-2} is very close
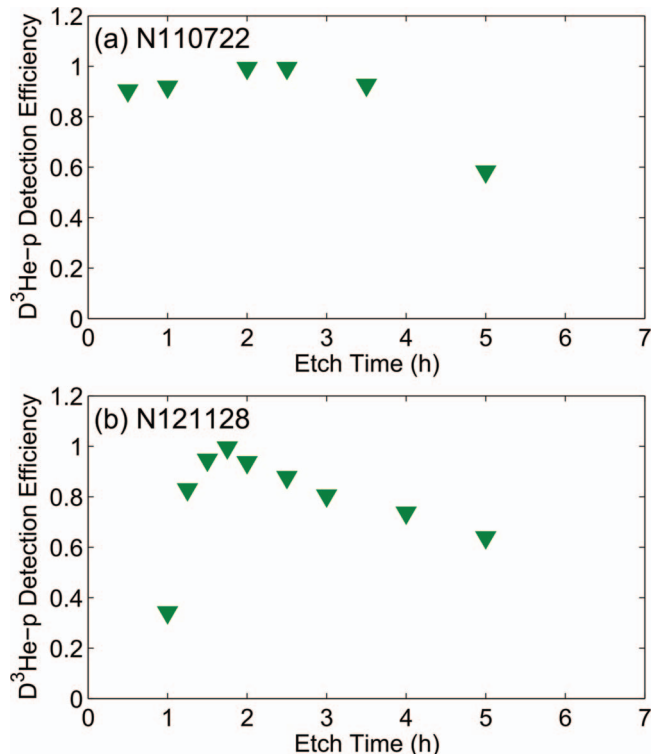

FIG. 6. WRF-inferred D^{3}He yields, normalized to the actual yields, as a function of etch time for (a) NIF shot N110722, at a fluence of 4.3×10^5 cm^{-2}, and (b) NIF shot N121128, at a fluence of 6.5×10^5 cm^{-2}. The protons contributing to the WRF analysis had an incident energy on the CR-39 of $\sim$1-4 MeV.

to the fluence upper-limit for being able to detect 100% of protons using the WRF. Under such conditions, the ability to reconstruct a proton spectrum and infer ion temperature and ρR is also impaired.

III. SCATTERING PINHOLE DETECTOR FOR EXTENSION OF PROTON YIELD UPPER LIMIT

As demonstrated in Figure 4(c), at a high enough fluence, above $\sim 3 \times 10^6$ cm^{-2} 2.4-MeV protons, track overlap begins to occur before all tracks are countable using standard processing techniques. To operate in such high-fluence conditions, as is occasionally necessary on experiments at NIF, the proton fluence at the CR-39 surface must be reduced.

A pinhole and scattering foil displaced $\sim$cm from the CR-39 can be utilized to reduce the fluence of protons at the CR-39 surface. The principle is illustrated schematically in Figure 7. Protons enter a small pinhole of diameter $d \sim 100$–300 μm, which at the fluences of interest ($\sim 10^6$ cm^{-2}) allow ~ 500–5000 protons to pass through. A thin foil immediately behind and attached to the pinhole substrate scatters protons at an average angle θ_s ($\sim 5^\circ$ for a 5 μm Ta foil). A spacer of length $L \sim$cm between the pinhole substrate and the CR-39 allows the protons to disperse over an area of radius $\sim L\theta_s$, such that the proton fluence at the CR-39 is lower than that at the pinhole by a factor of $\sim (L\theta_s/d)^2$. For $L \sim 1$ cm, the fluence at the CR-39 can be reduced by a factor of ~ 50.

This concept was tested on LEIA, which produced DD protons at a fluence of 1.3×10^6 cm^{-2} at the 200 μm-diameter pinhole. The resulting proton images on the CR-39, separated from the pinhole by 8.7 mm, are shown in Figure 8. Figure 8(a) shows that, in the absence of a scattering foil, the proton signal is highly concentrated over an area less than 1 mm at the center of the detector, at a fluence of 1.1×10^5 cm^{-2}. The finite size of the proton source reduces the fluence at the CR-39 to below that at the pinhole. The addition of a 5 μm Ta scattering foil behind the pinhole causes a noticeable difference in the proton signal at the CR-39 (Figure 8(b)). The proton signal is dispersed over several mm, such that the maximum fluence is reduced to 2.5×10^4 cm^{-2}, a factor of 50 lower than the incident fluence on the pinhole.

A version of the detector with a 300 μm diameter pinhole in a 150 μm-thick Al substrate and a 10 μm Ta scattering foil was fielded on D^{3}He exploding pusher shot
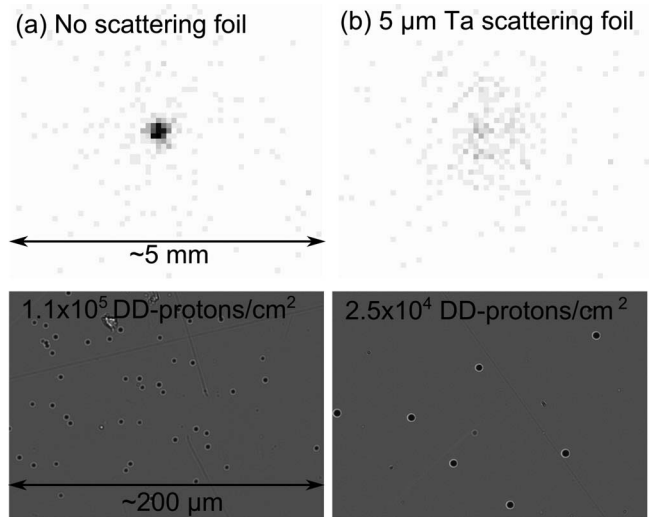
FIG. 8. Scattering pinhole data obtained on LEIA, (a) without a scattering foil, showing a fluence at the CR-39 of 1.1×10^5 DD-protons per cm^2, at a 1-h etch, and (b) with a 5 μm Ta scattering foil, resulting in a fluence of 2.5×10^4 DD-protons per cm^2 at the CR-39 at a 2-h etch. The incident fluence scales are identical in both images. The nominal proton fluence at the pinhole is 1.3×10^6 cm^{-2}, and is greater than that at the CR-39 in the no-foil case because of the finite size of the proton source. With the scattering foil, the fluence is reduced by a factor of 50 below that incident on the pinhole.

70400 on OMEGA, as depicted in Figure 9. The implosion produced 2.8×10^{10} DD protons as inferred from the DD-neutron yield measured by the neutron time of flight (nTOF) suite.[21] With the pinhole positioned 35.4 cm from the implosion, the fluence of DD protons incident at the pinhole was 1.8×10^6 cm^{-2}, such that a 100% detection efficiency would be nearly impossible using conventional CR-39 processing methods. The resulting DD-proton signal on the CR-39 after a 2-h etch shows a fairly diffuse signal spread over several mm (Figure 9(d)), much larger than the size of the pinhole, and roughly as expected based on a calculated mean scattering angle of $\sim 7^\circ$ and pinhole-CR-39 separation of 8.7 mm.[22] The maximum proton fluence was reduced from 1.8×10^6 cm^{-2} at the pinhole to 4.3×10^4 cm^{-2} at the CR-39, a factor of 40 reduction. The placement of the 10 μm Ta scattering foil 8.7 mm in front of the CR-39 did not result in a substantially different proton track diameter distribution than if the same 10 μm Ta foil were placed directly in front of the CR-39 (Figure 9(f)).

The total number of protons on the detector, as determined from the background-subtracted total under the peak in Figure 9, is 1240 ± 46 (Figure 9(e)), where the uncertainty is due to choices of subtraction of intrinsic background in the CR-39. The inferred DD-proton yield and its total uncertainty are determined as follows. The number N of protons on the CR-39 is used to determine the DD-p fluence F at the pinhole, as $F = N/(\pi(d/2)^2)$, where d is the diameter of the pinhole. The total yield is therefore $Y = F(4\pi R^2)$, where R is the distance from the implosion to the pinhole. Thus,

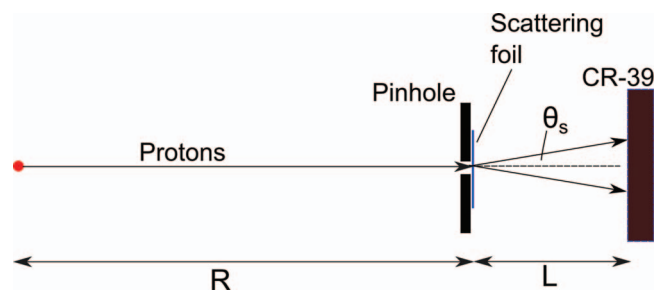$$Y = \frac{N}{\pi(d/2)^2} 4\pi R^2 \qquad (3)$$

FIG. 7. Pinhole plus scattering foil for reduction of proton fluence on the CR-39. Reducing the pinhole diameter, increasing the foil-CR-39 distance (L), and increasing the mean scattering angle θ_s all generate a greater fluence reduction factor.
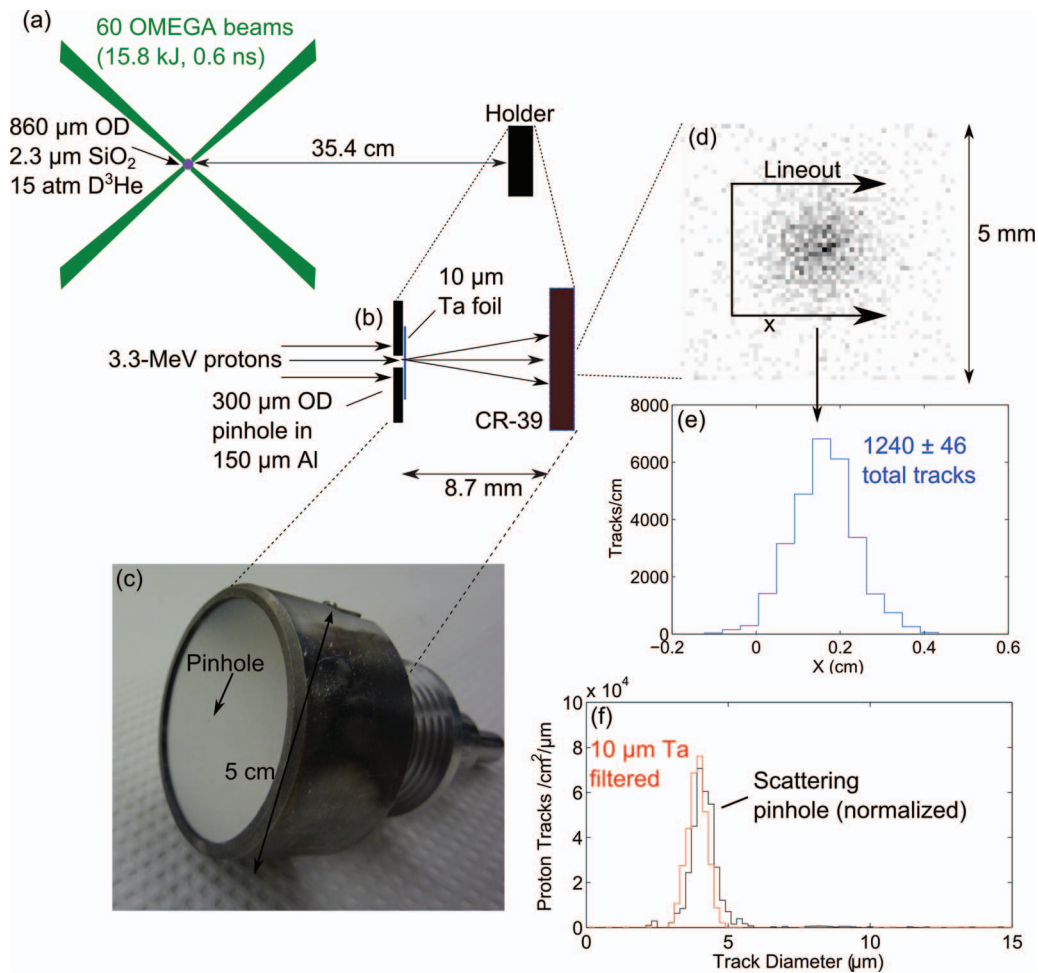
FIG. 9. Scattering pinhole setup and data obtained on OMEGA shot 70400. (a) The detector package was fielded 35.4 cm from an implosion of a thin glass capsule filled with D³He. (b) A 300 μm diameter pinhole followed by a 10 μm Ta foil was used to scatter 3.3-MeV protons produced in DD reactions onto the CR-39; (c) the detector package was housed inside the 5-cm diameter diagnostic module. The protons were dispersed (d) over an area several mm wide on the CR-39, reducing the incident fluence from 1.8×10^6 cm^{-2} at the pinhole to 4.3×10^4 cm^{-2} at the CR-39. The total number of tracks (e) was 1240 ± 46. It was found (f) that the distribution of proton diameters generated by the scattering pinhole instrument, using a 10 μm Ta scattering foil, is nearly identical to that produced by a detector with a simple 10 μm Ta filter directly in front of the CR-39 after a 2-h etch.

and the fractional uncertainty in the yield is

$$\frac{\Delta Y}{Y} = \sqrt{\left(\frac{\Delta N_{bkgd}}{N}\right)^2 + \left(\frac{\sqrt{N}}{N}\right)^2 + \left(2\frac{\Delta d}{d}\right)^2}, \qquad (4)$$

where the first term on the right-hand side represents the uncertainty due to intrinsic background, the second term represents the uncertainty due to raw counting statistics, and the third term represents the uncertainty in the pinhole diameter. The uncertainty in the distance from the pinhole to the implosion is <0.1% and can be neglected.

For $N = 1240$, $\Delta N_{bkgd} = 30$, $R = 35.4$ cm, $d = 300 \pm 10$ μm, $Y = 2.76 \pm 0.21 \times 10^{10}$, in excellent agreement with the nTOF-measured yield of 2.8×10^{10}. In this case, most of the yield uncertainty comes from uncertainty in the pinhole diameter (6.7% out of 7.6% total). For a smaller number of protons through the pinhole, the statistical and background-related uncertainties will be more significant.

IV. DISCUSSION AND APPLICATIONS

CR-39 proton data at energies of 1.7–4.3 MeV show that, in the absence of track overlap, 100% detection efficiency can be achieved under a 40× objective after as short as 0.75–2.5 h of etching in a 6N NaOH solution at 80 °C. The incident proton fluence limits the etch time for 100% detection, as track overlap limits the number of individual proton tracks that are counted correctly. For 2.0-MeV protons at a fluence of 2.0×10^5 cm^{-2}, track overlap becomes significant (<95% detection efficiency) after only 2 h of etching. Higher-energy protons that leave smaller tracks are slightly less susceptible to overlap, which only becomes significant for 4.3-MeV protons at 3.7×10^5 cm^{-2} after 5 h of etching. For 2.4-MeV protons at a fluence of 3×10^6 cm^{-2}, track overlap occurs even before all tracks can be counted, such that it is impossible to achieve 100% detection efficiency. This establishes the fluence upper-limit for 100% detection of individual 2.4-MeV-proton tracks.

For proton fluences where normal processing techniques cannot achieve 100% detection efficiency, a detector based on a pinhole and scattering foil has been designed to reduce

the fluence of protons incident on the CR-39 and effectively shift the range of operation of CR-39-based proton yield measurements. Proton fluences above the 100% efficiency limit are regularly achieved on D_2 exploding pusher experiments on NIF for calibration of DD-neutron diagnostics, where DD yields of up to 1×10^{12} produce proton fluences of 3×10^7 cm^{-2} at CR-39 detectors at a position 50 cm from the implosion, fixed due to hardware limitations. This fluence is well above that at which normal processing techniques can work. A scattering pinhole-based instrument, housed entirely within the module currently used for WRF proton spectrometers,[19] can reduce the proton fluence incident on the CR-39 by a factor of $\sim$50, to $\sim$6 $\times 10^5$ cm^{-2}, which at energies of 1.7–2.4 MeV can be measured at 100% efficiency (Figure 4). This technique can also be applied for measurements of more energetic D^3He protons or for alpha particles produced in D^3He or DT implosions, and future work may also apply this fluence reduction technique to proton spectral measurements using the WRF spectrometer.

V. CONCLUSIONS

Empirical studies have established a fluence upper limit for 100% detection efficiency of protons in CR-39 of $\lesssim 3 \times 10^6$ cm^{-2} for 2.4-MeV protons. At higher fluences, the onset significant track overlap – preventing individual tracks from being distinguished and properly counted – occurs at etch times short enough that the tracks are not entirely detectable and 100% detection efficiency is never achieved. At the OMEGA and NIF laser facilities, fixed diagnostic positions sometimes force CR-39-based diagnostics to be fielded at distances where the proton fluence can exceed this fluence upper limit. For such circumstances, a pinhole and scattering-foil has been developed and implemented to reduce the fluence of DD protons at the CR-39 surface by a factor of $\sim$40 or more. This detector package significantly extends the yield upper limit for DD-proton measurements on thin-shell implosions, and this technique can be further adapted to measurements of other fusion products.

[1]A. P. Fews and D. L. Henshaw, Nucl. Instrum. Methods Phys. Res. **197**, 517 (1982).

[2]D. G. Hicks, C. K. Li, F. H. Séguin, A. K. Ram, J. A. Frenje, R. D. Petrasso, J. M. Soures, V. Y. Glebov, D. D. Meyerhofer, S. Roberts, C. Sorce, C. Stoeckl, T. C. Sangster, and T. W. Phillips, Phys. Plasmas **7**, 5106 (2000).

[3]C. K. Li, D. G. Hicks, F. H. Séguin, J. A. Frenje, R. D. Petrasso, J. M. Soures, P. B. Radha, V. Y. Glebov, C. Stoeckl, D. R. Harding, J. P. Knauer, R. Kremens, F. J. Marshall, D. D. Meyerhofer, S. Skupsky, S. Roberts, C. Sorce, T. C. Sangster, T. W. Phillips, M. D. Cable, and R. J. Leeper, Phys. Plasmas **7**, 2578 (2000).

[4]F. H. Séguin, J. A. Frenje, C. K. Li, D. G. Hicks, S. Kurebayashi, J. R. Rygg, B. E. Schwartz, R. D. Petrasso, S. Roberts, J. M. Soures, D. D. Meyerhofer, T. C. Sangster, J. P. Knauer, C. Sorce, V. Y. Glebov, C. Stoeckl, T. W. Phillips, R. J. Leeper, K. Fletcher, and S. Padalino, Rev. Sci. Instrum. **74**, 975 (2003).

[5]J. A. Frenje, D. T. Casey, C. K. Li, J. R. Rygg, F. H. Séguin, R. D. Petrasso, V. Y. Glebov, D. D. Meyerhofer, T. C. Sangster, S. Hatchett, S. Haan, C. Cerjan, O. Landen, M. Moran, P. Song, D. C. Wilson, and R. J. Leeper, Rev. Sci. Instrum. **79**, 10E502 (2008).

[6]F. H. Séguin, J. L. DeCiantis, J. A. Frenje, C. K. Li, J. R. Rygg, C. D. Chen, R. D. Petrasso, J. A. Delettrez, S. P. Regan, V. A. Smalyuk, V. Y. Glebov, J. P. Knauer, F. J. Marshall, D. D. Meyerhofer, S. Roberts, T. C. Sangster, C. Stoeckl, K. Mikaelian, H. S. Park, H. F. Robey, and R. E. Tipton, Phys. Plasmas **13**, 082704 (2006).

[7]C. K. Li, F. H. Séguin, J. A. Frenje, J. R. Rygg, R. D. Petrasso, R. P. J. Town, P. A. Amendt, S. P. Hatchett, O. L. Landen, A. J. Mackinnon, P. K. Patel, V. A. Smalyuk, J. P. Knauer, T. C. Sangster, and C. Stoeckl, Rev. Sci. Instrum. **77**, 10E725 (2006).

[8]J. R. Rygg, F. H. Séguin, C. K. Li, J. A. Frenje, M. J.-E. Manuel, R. D. Petrasso, R. Betti, J. A. Delettrez, O. V. Gotchev, J. P. Knauer, D. D. Meyerhofer, F. J. Marshall, C. Stoeckl, and W. Theobald, Science **319**, 1223 (2008).

[9]C. K. Li, F. H. Séguin, J. A. Frenje, M. Rosenberg, R. D. Petrasso, P. A. Amendt, J. A. Koch, O. L. Landen, H. S. Park, H. F. Robey, R. P. J. Town, A. Casner, F. Philippe, R. Betti, J. P. Knauer, D. D. Meyerhofer, C. A. Back, J. D. Kilkenny, and A. Nikroo, Science **327**, 1231 (2010).

[10]A. B. Zylstra, J. A. Frenje, F. H. Séguin, M. G. Johnson, D. T. Casey, M. J. Rosenberg, C. Waugh, N. Sinenian, M. J.-E. Manuel, C. K. Li, R. D. Petrasso, Y. Kim, and H. W. Herrmann, Nucl. Instrum. Methods Phys. Res. A **681**, 84 (2012).

[11]G. Miller, E. Moses, and C. Wuest, Opt. Eng. **43**, 2841 (2004).

[12]T. R. Boehly, D. L. Brown, R. S. Craxton, R. L. Keck, J. P. Knauer, J. H. Kelly, T. J. Kessler, S. A. Kumpan, S. J. Loucks, S. A. Letzring, F. J. Marshall, R. L. McCrory, S. F. B. Morse, W. Seka, J. M. Soures, and C. P. Verdon, Opt. Commun. **133**, 495 (1997).

[13]T. Yamauchi, Radiat. Meas. **36**, 73 (2003).

[14]I. Rajta, E. Baradács, A. A. Bettiol, I. Csige, K. Tőkési, L. Budai, and A. Z. Kiss, Nucl. Instrum. Methods Phys. Res. B **231**, 384 (2005).

[15]S. Gaillard, J. Fuchs, N. R.-L. Galloudec, and T. E. Cowan, Rev. Sci. Instrum. **78**, 013304 (2007).

[16]The curve of proton track diameter as a function of incident proton energy has a similar shape to the curve of proton stopping power in CR-39, dE/dx as a function of proton energy E, though the empirically observed peak in the "diameter versus energy" curve occurs around $\sim$0.5 MeV, while the Bragg-peak energy for proton stopping in CR-39 is around $\sim$0.1 MeV.[4,22]

[17]N. Sinenian, M. J. Rosenberg, M. Manuel, S. C. McDuffee, D. T. Casey, A. B. Zylstra, H. G. Rinderknecht, M. G. Johnson, F. H. Séguin, J. A. Frenje, C. K. Li, and R. D. Petrasso, Rev. Sci. Instrum. **82**, 103303 (2011).

[18]N. Sinenian, M. J.-E. Manuel, A. B. Zylstra, M. Rosenberg, C. J. Waugh, H. G. Rinderknecht, D. T. Casey, H. Sio, J. K. Ruszczynski, L. Zhou, M. G. Johnson, J. A. Frenje, F. H. Séguin, C. K. Li, R. D. Petrasso, C. L. Ruiz, and R. J. Leeper, Rev. Sci. Instrum. **83**, 043502 (2012).

[19]F. H. Séguin, N. Sinenian, M. Rosenberg, A. Zylstra, M. J.-E. Manuel, H. Sio, C. Waugh, H. G. Rinderknecht, M. G. Johnson, J. Frenje, C. K. Li, R. Petrasso, T. C. Sangster, and S. Roberts, Rev. Sci. Instrum. **83**, 10D908 (2012).

[20]A. B. Zylstra, J. A. Frenje, F. H. Séguin, M. J. Rosenberg, H. G. Rinderknecht, M. G. Johnson, D. T. Casey, N. Sinenian, M. J.-E. Manuel, C. J. Waugh, H. W. Sio, C. K. Li, R. D. Petrasso, S. Friedrich, K. Knittel, R. Bionta, M. McKernan, D. Callahan, G. W. Collins, E. Dewald, T. Doppner, M. J. Edwards, S. Glenzer, D. G. Hicks, O. L. Landen, R. Lonson, A. Mackinnon, N. Meezan, R. R. Prasad, J. Ralph, M. Richardson, J. R. Rygg, S. Sepke, S. Weber, R. Zacharias, E. Moses, J. Kilkenny, A. Nikroo, T. C. Sangster, V. Glebov, C. Stoeckl, R. Olson, R. J. Leeper, J. Kline, G. Kyrala, and D. Wilson, Rev. Sci. Instrum. **83**, 10D901 (2012).

[21]V. Y. Glebov, C. Stoeckl, T. C. Sangster, S. Roberts, G. J. Schmid, R. A. Lerche, and M. J. Moran, Rev. Sci. Instrum. **75**, 3559 (2004).

[22]J. F. Ziegler, M. D. Ziegler, and J. P. Biersack, Nucl. Instrum. Methods Phys. Res. B **268**, 1818 (2010).